J|A|C|S ARTICLES

Published on Web 12/22/2009

Uncovering Individual Hydrogen Bonds in Rotaxanes by Frequency Shifts

Barbara Kirchner,*,† Christian Spickermann,† Werner Reckien,† and Christoph A. Schalley‡

Lehrstuhl für Theoretische Chemie, Wilhelm-Ostwald Institut für Physikalische und Theoretische Chemie, Universität Leipzig, Linnéstr. 2, D-04103 Leipzig, Germany, and Organische Chemie, Institut für Chemie und Biochemie, Freie Universität Berlin, Takusstrasse 3, D-14195 Berlin, Germany

Received April 9, 2009; E-mail: bkirchner@uni-leipzig.de

Abstract: We present a theoretical investigation of amide pseudorotaxane IR spectra in the harmonic approximation. In particular, we focus on the effect of axle substitution on the hydrogen bonds that are formed between axle and wheel. Two types of pseudorotaxanes are studied: one with the substituent affecting mostly the axle's carbonyl group and one with the effect influencing primarily the amide NH group. Sizeable red shifts are predicted for the carbonyl stretching frequencies, and large red shifts for the NH stretching frequencies. For the wheel amide groups involved in hydrogen bonding merely with their NH hydrogens, a small shift is observed for the carbonyl stretch mode. A clear relation is observed between the NH stretch shifts and individual hydrogen bond energies. This is confirmed by correlations of the shared electron number with the NH stretch shift showing that this quantity can be taken as an indicator for individual hydrogen bond energies. Axle substitution influences the strengths of the individual hydrogen bonds which is again reflected in the NH stretch frequency shifts. A linear relationship of Hammett's substituent parameters with the NH frequency shifts can be established.

1. Introduction

Rotaxanes are a particularly interesting class of supramolecules. They consist of an axle, which is threaded into a macrocyclic wheel. The dethreading of the axle is usually inhibited by bulky stopper groups. One of the most interesting features of such interlocked molecules is their mechanical bond. Although both components are not covalently connected with each other, a covalent bond needs to be broken in order to separate them.[1,2] Because of the mechanical bond, the two components of a rotaxane are able to move quite freely with respect to each other, even though dissociation is impossible. Nevertheless, noncovalent bonds may have a decisive effect on the movement of the wheel along the linear part of the rotaxane. In particular, hydrogen bonding between axle and wheel can be used to control the relative motions in rotaxanes.[3−18] If this principle is used in a clever way, molecular shuttles[19] can be constructed in which the wheel shifts from one hydrogen bonding station on the axle to another one. This process can even be triggered by different external stimuli such as light, redox processes, or chemical signals such as pH gradients.[3,4,8,9,11,12,16,18,20] Most rotaxane syntheses use noncovalent template effects which direct an axle-center piece or a semiaxle into the macrocyclic wheel by precisely preorganized nonco-

† Universität Leipzig.
‡ Freie Universität Berlin.

(1) Schill, G. *Rotaxanes and Knots*; Academic Press: New York, 1971.
(2) Sauvage, J. P.; Dietrich-Buchecker, C., Eds.; *Molecular Catenanes, Rotaxanes, and Knots*; Wiley-VCH: Weinheim, 1999.
(3) Umehara, T.; Kawai, H.; Fujiwara, K.; Suzuki, T. *J. Am. Chem. Soc.* **2008**, *130*, 13981–13988.
(4) Fioravanti, G.; Haraszkiewicz, N.; Kay, E. R.; Mendoza, S. M.; Bruno, C.; Marcaccio, M.; Wiering, P. G.; Paolucci, F.; Rudolf, P.; Brouwer, A. M.; Leigh, D. A. *J. Am. Chem. Soc.* **2008**, *130*, 2593–2601.
(5) Baytekin, B.; Zhu, S. S.; Brusilowskij, B.; Illigen, J.; Ranta, J.; Huuskonen, J.; Russo, L.; Rissanen, K.; Kaufmann, L.; Schalley, C. A. *Chem.—Eur. J.* **2008**, *14*, 10012–10028.
(6) Haussmann, P. C.; Khan, S. I.; Stoddart, J. F. *J. Org. Chem.* **2007**, *72*, 6708–6713.
(7) Vickers, M. S.; Beer, P. D. *Chem. Soc. Rev.* **2007**, *36*, 211–225.
(8) Marlin, D. S.; Cabrera, D. G.; Leigh, D. A.; Slawin, A. M. Z. *Angew. Chem., Int. Ed.* **2006**, *45*, 1385–1390; *Angew. Chem.* **2006**, *118*, 1413−1418.
(9) Kay, E. R.; Leigh, D. A. *Top. Curr. Chem.* **2005**, *262*, 133–177.
(10) Moonen, N. N. P.; Flood, A. H.; Fernandez, J. M.; Stoddart, J. F. *Top. Curr. Chem.* **2005**, *262*, 99–132.
(11) Ghosh, P.; Federwisch, G.; Kogej, M.; Schalley, C. A.; Haase, D.; Saak, W.; Lützen, A.; Gschwind, R. M. *Org. Biomol. Chem.* **2005**, *3*, 2691–2700.
(12) Keaveney, C. M.; Leigh, D. A. *Angew. Chem., Int. Ed.* **2004**, *43*, 1222–1224; *Angew. Chem.* **2004**, *116*, 1242−1244.
(13) Schalley, C. A.; Weilandt, T.; Brüggemann, J.; Vögtle, F. *Top. Curr. Chem.* **2004**, *248*, 141–200.
(14) Schalley, C.; Reckien, W.; Peyerimhoff, S.; Baytekin, B.; Vögtle, F. *Chem.—Eur. J.* **2004**, *10*, 4777–4789.
(15) Tseng, H. R.; Vignon, S. A.; Celestre, P. C.; Perkins, J.; Jeppesen, J. O.; Fabio, A. D.; Ballardini, R.; Gandolfi, M. T.; Venturi, M.; Balzani, V.; Stoddart, J. F. *Chem.—Eur. J.* **2004**, *10*, 155–172.
(16) Brouwer, A. M.; Fazio, S. M.; Frochot, C.; Gatti, F. G.; Leigh, D. A.; Wong, J. K. Y.; Wurpel, G. W. H. *Pure Appl. Chem.* **2003**, *75*, 1055–1060.
(17) Linnartz, P.; Bitter, S.; Schalley, C. A. *Eur. J. Org. Chem.* **2003**, *24*, 4819–4829.
(18) Alteri, A.; Gatti, F. G.; Kay, E. R.; Leigh, D. A.; Martel, D.; Paolucci, F.; Slawin, A. M. Z.; Wong, J. K. Y. *J. Am. Chem. Soc.* **2003**, *125*, 8644–8654.
(19) Anelli, P. L.; Spencer, N.; Stoddart, J. F. *J. Am. Chem. Soc.* **1991**, *113*, 5131–5133.
(20) Balzani, V.; Venturi, M.; Credi, A. *Molecular Devices and Machines*; Wiley-VCH: Weinheim, 2003.

10.1021/ja902628n

valent bonds.[13,21−25] The resulting pseudorotaxane can then be equipped with the stopper groups to fix the interlocked topology.

Recently, Buma and co-workers published the first spectroscopic study of isolated mechanically interlocked molecules in the gas phase, i.e., in the absence of disturbing solvent-molecule interactions.[26] Before the work of Buma et al., these systems have been investigated spectroscopically in the presence of solvent molecules. For example, Larsen et al. studied the detailed structure of rotaxanes in $CHCl_3$ with time-resolved two-dimensional IR studies.[27] Jagesar et al. measured and calculated the IR spectrum of a rotaxane and its shuttling process in solvents with different polarities.[28] Jimenez et al. studied the effects that the solvent exerts on the end-capping process of a pseudorotaxane.[29] High resolution UV spectra were used to understand the functionality of rotaxane molecules.[30] The rotaxanes investigated by Buma et al. contain two types of carbonyl groups.[26] One of them is located at the macrocycle not directly taking part in the axle−wheel interaction. The other links axle and wheel noncovalently through hydrogen bonding. Midinfrared spectroscopy detects the formation of the hydrogen-bonded complex between both components through a red shift of the carbonyl stretching vibration of the carbonyl group directly involved in hydrogen bonding. Furthermore, also the macrocycle's non-hydrogen-bonded carbonyl group vibration undergoes a shift upon complex formation. These highly interesting results prompted us to investigate in detail the calculated vibrational spectra of amide pseudorotaxanes whose binding energies formed the focus of an earlier combined theoretical and experimental study[31] and of another species not studied by us before.

A wealth of experimental and theoretical data on hydrogen bonding in general and between amide groups especially is available in literature; cf. e.g. refs 32−38. For an excellent overview, see ref 39. In this context it is important to mention that cooperativity has been detected experimentally in CO stretching frequencies as well as theoretically from different calculations.[32,33,37,38] Herrebout et al.[40] investigated the vibrational spectrum of *N*-methylacetamide in different environments and aggregate states and discussed cooperative effects with the aid of calculated fundamentals for differently sized clusters.[40] Recently, Suhm and co-workers presented an excellent overview of the field of spectroscopic amide hydrogen-bonding studies in their report on direct absorption vibrational data of four simple amides in vacuo.[39] For these amide-containing molecules, Suhm and co-workers investigated the amide-I (CO) and the amide-A (NH) bands and found non-*N*-methylated amides to form symmetric dimers, whereas singly *N*-methylated amides form only singly hydrogen-bonded dimers.[39] Among the available theoretical studies on supramolecular systems,[41,42] several reports on (pseudo)rotaxanes or similar complexes exist. Detailed studies of the formation of amide rotaxanes and the hydrogen-bonding motifs mediating the threading of the axle through the wheel were reported earlier by us.[14,43−45]

In the following, we will first briefly discuss the computational methodologies and the systems investigated[31] followed by an analysis of the calculated spectra and the substituent-induced frequency shifts. Finally, correlations of the individual hydrogen-bond energies with the frequency shifts of the NH stretch modes are examined. Then, the total interaction energies are correlated with the frequency shifts. A plot of the frequency shifts of the NH stretch vibration over Hammett's substituent parameters[46] concludes the results section.

2. Computational Methodologies

For all compounds the structures were optimized in C_1 symmetry. The Leigh-type pseudorotaxanes were additionally optimized in C_{2h} symmetry to explore the symmetry behavior of their spectra. Density functional theory (DFT) with the gradient-corrected functional BP86 combined with the resolution of identity technique (RI) and the TZVP basis set was applied.[47,48] All calculations for the previously investigated pseudorotaxanes (Vögtle-type; see Figure 1 upper panel) were performed using the Turbomole 5.5 program package; the second type of rotaxane (Leigh-type; see Figure 1 lower panel) was studied with the newer Turbomole 5.10 program package.[47] Interaction energies were counterpoise-corrected by the procedure introduced by Boys and Bernardi.[49] The adiabatic complex interaction energies ΔE^{calc} were calculated according to the supramolecular approach by subtracting the energies of the relaxed monomers $E^{\text{relax}}_{\text{wheel}}$, $E^{\text{relax}}_{\text{guest}}$, and the basis set superposition error (BSSE) contributions from the total cluster energy E^{tot}.[50,51]

$$\Delta E^{\text{calc}} = E^{\text{tot}} - E^{\text{relax}}_{\text{wheel}} - E^{\text{relax}}_{\text{guest}} - \Delta E_{\text{BSSE}} \qquad (1)$$

The BSSE does not exceed 10 kJ/mol for any of the complexes calculated.

(21) Hoss, R.; Vögtle, F. *Angew. Chem., Int. Ed. Engl.* **1994**, *33*, 375–384; *Angew. Chem.* **1994**, *106*, 389−398.
(22) Seel, C.; Parham, A. H.; Safarowsky, O.; Hübner, G. M.; Vögtle, F. *J. Org. Chem.* **1999**, *64*, 7236–7242.
(23) Vögtle, F.; Dünnwald, T.; Schmidt, T. *Acc. Chem. Res.* **1996**, *29*, 451–560.
(24) Vögtle, F.; Händel, M.; Meier, S.; Ottens-Hildebrandt, S.; Ott, F.; Schmidt, T. *Liebig. Ann.* **1994**, 739–743.
(25) Reuter, C.; Schmieder, R.; Vögtle, F. *Pure Appl. Chem.* **2000**, *72*, 2233–2241.
(26) Rijs, A. M.; Compagnon, I.; Oomens, J.; Hannam, J. S.; Leigh, D. A.; Buma, W. J. *J. Am. Chem. Soc.* **2009**, *131*, 2428–2429.
(27) Larsen, O. F. A.; Bodis, P.; Buma, W. J.; Hannam, J. S.; Leigh, D. A.; Woutersen, S. *Proc. Natl. Acad. Sci. U.S.A.* **2005**, *102*, 13378–13382.
(28) Jagesar, D. C.; Hartl, F.; Buma, W. J.; Brouwer, A. M. *Chem.−Eur. J.* **2008**, *14*, 1935–1946.
(29) Jimenez, R.; Martin, C.; Lopez-Cornejo, P. *J. Phys. Chem. B* **2008**, *112*, 11610–11615.
(30) Rijs, A. M.; Crews, B. O.; de Vries, M. S.; Hannam, J. S.; Leigh, D. A.; Fanti, M.; Zerbetto, F.; Buma, W. J. *Angew. Chem., Int. Ed.* **2008**, *47*, 3174–3179; *Angew. Chem.* **2008**, *120*, 3218−3223.
(31) Spickermann, C.; Felder, T.; Schalley, C. A.; Kirchner, B. *Chem.−Eur. J.* **2008**, *14*, 1216–1227.
(32) Kobko, N.; Paraskevas, L.; del Rio, E.; Dannenberg, J. *J. Am. Chem. Soc.* **2001**, *123*, 4348–4349.
(33) Wieczorek, R.; Dannenberg, J. *J. Am. Chem. Soc.* **2003**, *125*, 14065–14071.
(34) Dunn, M.; Pokon, E.; Shields, G. *J. Am. Chem. Soc.* **2004**, *126*, 2647–2653.
(35) Alongi, K.; Dibble, T.; Shields, G.; Kirschner, K. *J. Phys. Chem. A* **2006**, *110*, 3686–3691.
(36) Todorova, T.; Seitsonen, A.; Hutter, J.; Kuo, I.; Mundy, C. *J. Phys. Chem. B* **2006**, *110*, 3685–3691.
(37) Kobko, N.; Dannenberg, J. J. *J. Phys. Chem. A* **2003**, *107*, 6688–6697.
(38) Chen, Y.; Viswanathan, R.; Dannenberg, J. J. *J. Phys. Chem. B* **2007**, *111*, 8329–8334.
(39) Albrecht, M.; Rice, C. A.; Suhm, M. A. *J. Phys. Chem. A* **2008**, *112*, 7530–7542.
(40) Herrebout, W. A.; Clou, K.; Desseyn, H. O. *J. Phys. Chem. A* **2001**, *105*, 4865–4881.
(41) Kirchner, B.; Reiher, M. Theoretical Methods in Supramolecular Chemistry. In *Analytical Methods for Supramolecular Chemistry*; Schalley, C. A., Ed.; Wiley-VCH: Weinheim, 2006.
(42) Hurley, M.; Hammes-Schiffer, S. *J. Phys. Chem. A* **1997**, *101*, 3977–3989.
(43) Reckien, W.; Peyerimhoff, S. D. *J. Phys. Chem. A* **2003**, *107*, 9634–9640.
(44) Reckien, W.; Kirchner, B.; Peyerimhoff, S. D. *J. Phys. Chem. A* **2006**, *110*, 12963–12970.
(45) Reckien, W.; Spickermann, C.; Eggers, M.; Kirchner, B. *Chem. Phys.* **2008**, *343*, 186–199.

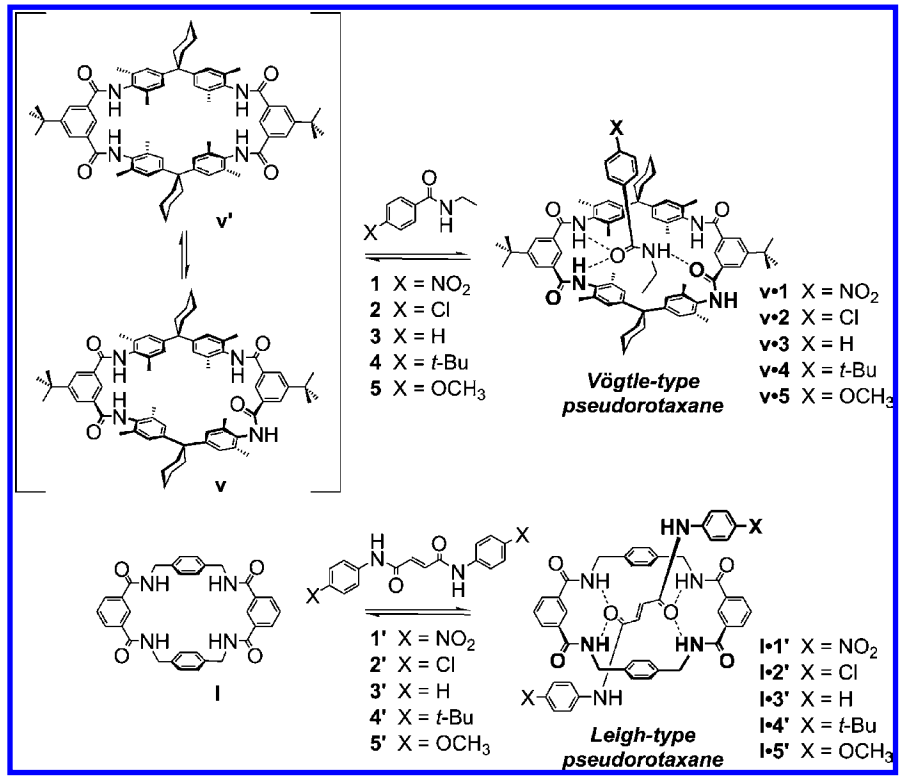

Figure 1. Chemical structure of the systems investigated. Upper panel: Vögtle-type pseudorotaxane. Lower panel: Fumaramide[2] pseudorotaxane which will be denoted Leigh-type rotaxane.

Furthermore, the computation of the shared electron numbers (SENs) was carried out.[52] The determination of the two-center SEN values and the computation of partial charges were based on the Davidson population analysis.[53] In the SEN approach the linear relationship between the two-center shared electron number of a hydrogen bond and its binding energy allows an estimation of the bond strength if the parameters m and b of the corresponding linear equation are known[52,54,55]

$$E^{\mathrm{SEN}} = m\sigma_{\mathrm{HA}} + b \qquad (2)$$

where σ_{HA} denotes the two-center SEN between the donor hydrogen atom H and the acceptor atom A, m gives the value of the slope, and b is the axis intercept of the linear equation. This procedure was already used for a broad variety of chemical applications concerning hydrogen bonding.[52,54,50] The slope parameter m depends on the acceptor atom of the hydrogen bond and was determined for a wide range of hydrogen bonds involving large numbers of different atoms in previous work.[55] In the present application, the values $m = -724$ kJ/(mol e) and $b = 2.01$ kJ/mol are chosen in agreement with amide-type hydrogen bonds and the BP86/TZVP combination.[44] Values for the total hydrogen-bond energy in terms of the SEN method are obtained by summing up the energies of all hydrogen bonds in the complex. It should be mentioned briefly that due to the wrong description of dispersion in density functional theory and due to the choice of a finite basis set, errors could have been introduced which were discussed in a previous article.[45]

For the frequency analyses in the harmonic approximation, the program package SNF was employed.[56] The second derivatives of the total energy were calculated as numerical derivatives of the gradients. The numerical accuracy of the calculated wave numbers in this approach is not below 1 cm^{-1}. To illustrate the calculated spectra, a half width of 5 cm^{-1} is chosen and each spectrum is convoluted in Lorentzians. We neither applied scaling factors for a readjustment of the calculated frequencies nor considered anharmonic effects. Such effects, for example nuclear quantum effects for the proton transfer or isotope effects, have been broadly studied by the group of Hammes-Schiffer.[42,57,58] For example, the weakening (bond elongation) of the hydrogen bonding in several examples upon deuteration is excellently discussed and studied in ref 57. For a series of small molecules including protons, the presented calculations showed that increasing the mass of the light atom decreases the bond length between proton and donor atom.[57] Furthermore, it was found that the zero-point energy is larger for the smaller mass (proton instead of deuterium or tritium). As a result this leads to more significant anharmonic effects and thus to a greater average bond length.[57] For the Leigh-type complexes, Raman spectra were calculated. Due to the computational resources we did not change the basis set for these calculations. Further computational details can be found in ref 59.

(46) Hammett, L. *J. Am. Chem. Soc.* **1937**, *59*, 96–103.
(47) Ahlrichs, R.; Bär, M.; Häser, M.; Horn, H.; Kölmel, C. *Chem. Phys. Lett.* **1989**, *162*, 165–169. Current version: see http://www.turbomole.de.
(48) Becke, A. D. *Phys. Rev. A* **1988**, *38*, 3098–3100.
(49) Boys, S. F.; Bernardi, F. *Mol. Phys.* **1970**, *19*, 553–566.
(50) Kossmann, S.; Thar, J.; Kirchner, B.; Hunt, P. A.; Welton, T. *J. Chem. Phys.* **2006**, *124*, 174506.
(51) Kirchner, B.; Reiher, M. *J. Am. Chem. Soc.* **2002**, *124*, 6206–6215.
(52) Reiher, M.; Sellmann, D.; Hess, B. A. *Theor. Chem. Acc.* **2001**, *106*, 379–392.
(53) Davidson, E. R. *J. Chem. Phys.* **1967**, *46*, 3320–3324.
(54) Reiher, M.; Kirchner, B. *J. Phys. Chem. A* **2003**, *107*, 4141–4146.
(55) Thar, J.; Kirchner, B. *J. Phys. Chem. A* **2006**, *110*, 4229–4237.
(56) Neugebauer, J.; Reiher, M.; Kind, C.; Hess, B. A. *J. Comput. Chem.* **2002**, *23*, 895–910.
(57) Reyes, A.; Pak, M. V.; Hammes-Schiffer, S. *J. Chem. Phys.* **2005**, *123*, 064104.
(58) Carra, C.; Irdanova, N.; Hammes-Schiffer, S. *J. Phys. Chem. B* **2002**, *106*, 8415–8421.
(59) Reiher, M.; Brehm, G.; Schneider, S. *J. Phys. Chem. A* **2004**, *108*, 734–742.

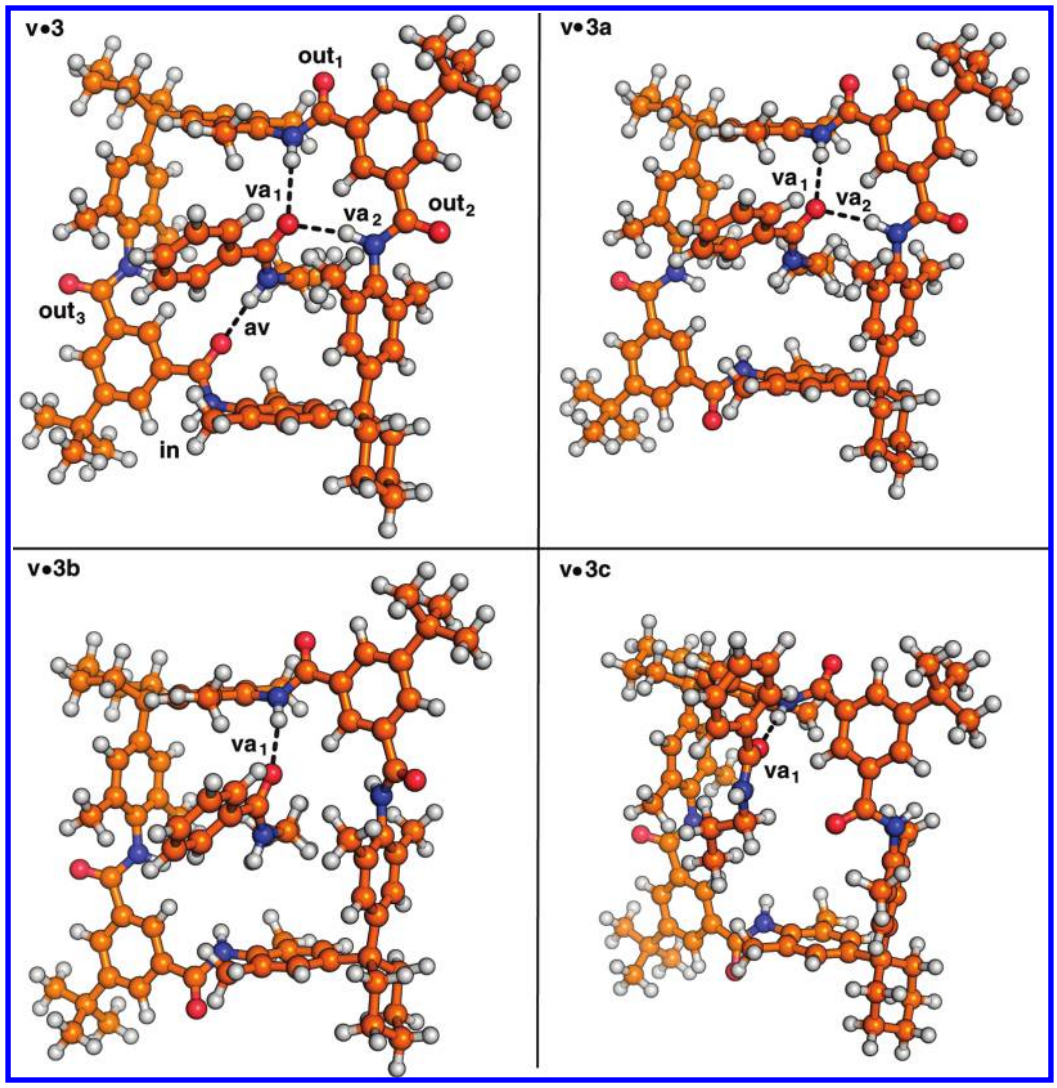

Figure 2. Upper left: Ball and stick model of the calculated geometry of **v•3**. Labels va_1, va_2, av identify the individual hydrogen bonds. The other Vögtle-type complexes form an analogous binding pattern as **v•3**. The remaining panels show ball and stick models of different coconformations of the threading process. Later on these coconformations of **v•3** will be utilized for a linear regression analysis.

3. Structures under Study

As shown in Figure 1 upper panel, the previously investigated pseudorotaxanes are formed by binding of an amide axle inside the cavity of a tetralactam macrocycle. This pseudorotaxane will be denoted Vögtle-type pseudorotaxane throughout the article.[13,21−25]

Figure 1 (lower panel) also shows the second type of rotaxanes subject to this study. The benzylic amide macrocycle contains two isophtalamide units. The axle consists of a fumaramide moiety. Because of the functional groups involved, this kind of rotaxanes can form four wheel-NH···O═C-axle hydrogen bonds. This pseudorotaxane will be denoted Leigh-type pseudorotaxane throughout the article.[9,30] An important difference in addition to the molecular composition of the two pseudorotaxanes consists in the influence of the substituent effect. While the substituent is conjugated through the aromatic ring with the axle carbonyl group in the Vögtle-type pseudorotaxanes, it affects primarily the amide NH group in the Leigh-type pseudorotaxanes.

The first type of pseudorotaxanes (Vögtle-type) comprises the structures **v•1** to **v•5** and their components, i.e. wheel **v** and axles **1** to **5**; see Figure 1 upper panel.[31] These complexes can be considered as pseudorotaxanes, because the hydrogen bonds connecting the two components also define the threaded orientation of the axle inside the wheel. The formal addition of two stoppers would lead to the well-known family of Vögtle-type amide rotaxanes.[60] While the wheel consists of a tetralactam macrocycle with four secondary amide groups, all axles exhibit a central benzoylamide group with different functional groups at the *para* position of the phenyl ring. In the pseudorotaxanes the macrocycle adopts a conformation in which three amide carbonyl groups point away from the cavity (out conformation) and one points inward (in conformation); see also Figure 2.

Upon complex formation with the axle amide, three relatively strong hydrogen bonds are formed. The axle accepts two hydrogen bonds with its carbonyl group (va_1 and va_2) and donates its NH group to the inward pointing carbonyl group (av).[31,44] All pseudorotaxanes have the same coconformation, i.e., the same relative positions of the noncovalently bound components with respect to each other.[27] The substituent effects of functional groups on hydrogen bonds are well-known and

(60) Jäger, R.; Vögtle, F. *Angew. Chem., Int. Ed.* **1997**, *36*, 930–944; *Angew. Chem.* **1997**, *109*, 966−980.

Table 1. Vögtle-Type Complexes with Different Substituents and Corresponding Effects[a]

				individual hydrogen bond energy			total interaction energy		free energy
	group	main substituent effect	Hammett parameter σ	E_{av}^{SEN}	$E_{va_1}^{SEN}$	$E_{va_2}^{SEN}$	ΔE^{calc}	ΔE_{ZPE}^{calc}	ΔG^{calc}
v•1	NO_2	−M	−0.72	−16.0	−13.0	−3.8	−35.7	−32.6	25.1
v•2	Cl	−I	−0.17	−14.8	−14.4	−4.4	−36.6	−33.9	22.4
v•3	H	−	0	−13.9	−14.4	−4.6	−36.5	−33.9	22.2
v•4	*t*Bu	+I	0.23	−13.4	−14.4	−5.0	−36.0	−34.6	21.3
v•5	OCH_3	+M	0.30	−13.1	−15.8	−5.2	−37.9	−35.8	19.3

[a] The Hammett parameters σ are also listed. These parameters can be obtained easily from the difference of the pKa-values of the substituted benzoic acid minus the unsubstituted benzoic acid. Hydrogen bond energies for av, va_1 and va_2 are given next, for labels see Figure 2 together with the total interaction energy ΔE^{calc} including zero-point energy correction ΔE_{ZPE}^{calc} and the free energies of binding from ref 31. All energies in [kJ/mol].

have been studied extensively for example for the Watson−Crick-type base pairs.[61−63]

The individual hydrogen bond energies were obtained from a semiquantitative shared electron number (SEN) analysis (see Table 1).[55,64,65] While the av and the va_1 hydrogen bonds are approximately of similar strengths, the va_2 hydrogen bond is approximately one-third of their strength. The 2-fold hydrogen bond with its two hydrogen donor contributions (va_1 + va_2) is stronger than the single hydrogen bond av. Although the trend is small, all individual hydrogen bonds correlate well with the substituent effects as expressed in the Hammett σ -values. Only very small trends are visible in the total interaction energies with and without zero-point energy correction. Consequently, a detailed examination of the amide template effect requires ways to accurately describe the separate contributions from the *individual* hydrogen bonds. The free energies of binding in Table 1 are gas-phase values according to the rigid-rotor-harmonic-oscillator approximation. Solvent effects and a comparison with experimental data were reported previously.[31]

Electron donating substituents such as methoxy in **v•5** increase the electron density at the carbonyl oxygen and therefore strengthen the hydrogen bonds to this group; see $E_{va_1}^{SEN}$ and $E_{va_2}^{SEN}$ in Table 1. In this column the strongest hydrogen bonds va_1 and va_2 (CO) are found for the OCH_3 substituent in **v•5**. Vice versa the NH donor strength is significantly reduced; see E_{av}^{SEN} in Table 1.[44] Both effects cancel each other more or less completely (see Table 1), so that the overall binding energy is not affected much.[31] However, the strength of the individual hydrogen bonds clearly correlates with the substituent effects. It will thus be interesting to see whether these effects are detectable in the vibrational spectra.

The second type of pseudorotaxanes investigated are the structures **l•1′** to **l•5′** and their components, i.e. wheel **l** and axles **1′** to **5′**; see Figure 1 lower panel.[66] These interlocked molecules were widely studied and synthesized in the Leigh group (Figure 3).[12,67,68]

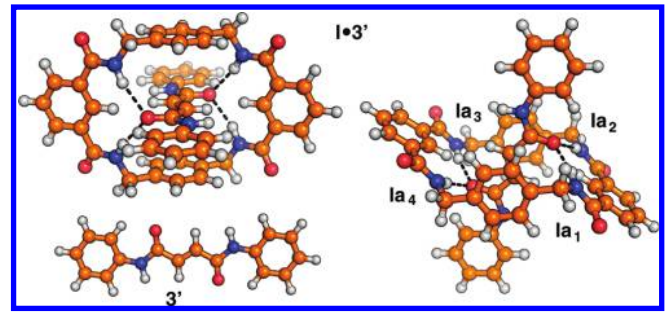

Figure 3. Ball and stick model of the calculated geometry of **l•3′** and structure of **3′** (lower left). Labels la_1, la_2, la_3, la_4 identify the individual but equivalent hydrogen bonds. The other complexes form an analogous binding pattern.

Table 2. Leigh-Type Complexes (C_{2h} Symmetry) with Different Substituents[a]

		σ_{HO}	E^{SEN}	$\sum_{i=1}^{4} E_i^{SEN}$	ΔE^{calc}	ΔE_{ZPE}^{calc}	ΔG^{calc}
l•1′	NO_2	0.0121	−6.8	−27.2	−35.7	−29.5	34.6
l•2′	Cl	0.0149	−8.8	−35.2	−46.4	−39.0	29.3
l•3′	H	0.0156	−9.3	−37.2	−51.4	−43.9	21.2
l•4′	*t*Bu	0.0161	−9.6	−38.4	−54.2	−46.7	18.1
l•5′	OCH_3	0.0175	−10.7	−42.8	−56.4	−47.8	21.7

[a] The shared electron numbers σ_{HO} in [*e*], the individual hydrogen bond energies E^{SEN}, the total interaction energy ΔE^{calc} including zero-point energy correction ΔE_{ZPE}^{calc}, and the free energy changes are given. Please note that due to the symmetry all four hydrogen bond are equivalent. Therefore only one value is given. All energies in [kJ/mol].

As in the case of the Vögtle-type pseudorotaxanes, substitution patterns are studied for this species. Table 2 lists some energetic data.

The individual hydrogen bonds in the symmetrical Leigh-type complexes are weaker than the strongest individual hydrogen bonds in the Vögtle-type complexes. However, the total interaction energies are up to 20 kJ/mol larger in the former pseudorotaxanes than in the latter. Thus these pseudorotaxanes might be more stable than the others at least from an energetic point of view. The zero-point energy correction is approximately of the same size in both complexes. The substitution trend is now apparent due to the lack of counter-balancing effects in the Leigh-type pseudorotaxanes and due to the fact that both sides of the axle contain the functional groups. This reveals energetic differences ranging up to 20 kJ/mol; compare the NO_2-species with the OCH_3-substituted complex in Table 2.

The symmetry of the Leigh-type complexes is also reflected in the geometry of the individual hydrogen bonds listed in Table 3. For example the deviation of the distances within a complex is less than 3 pm which is well within the error limit of the applied theoretical method.

(61) Kawahara, S.; Uchimaru, T.; Taira, K.; Sekine, M. *J. Phys. Chem. A* **2001**, *105*, 3894–3898.
(62) Kawahara, S.; Kobori, A.; Sekine, M.; Taira, K.; Uchimaru, T. *J. Phys. Chem. A* **2001**, *105*, 10596–10601.
(63) Kawahara, S.; Wada, T.; Kawauchi, S.; Uchimaru, T.; Sekine, M. *J. Phys. Chem. A* **1999**, *103*, 8516–8523.
(64) Reiher, M.; Kirchner, B. *J. Phys. Chem. A* **2003**, *107*, 4141–4146.
(65) Kirchner, B. *Phys. Rep.* **2007**, *1−3*, 1–111.
(66) Kay, E.; Leigh, D. A.; Zerbetto, F. *Angew. Chem., Int. Ed.* **2006**, *46*, 72–191; *Angew. Chem.* **2006**, *119*, 72−196.
(67) Lane, A. S.; Leigh, D. A.; Murphy, A. *J. Am. Chem. Soc.* **1997**, *119*, 11092–11093.
(68) Gatti, F. G.; Leigh, D. A.; Nepogodiev, S. A.; Slawin, A. M. Z.; Teat, S. J.; Wong, J. K. Y. *J. Am. Chem. Soc.* **2001**, *123*, 5983–5989.

Table 3. Leigh-Type Complexes (C_{2h} Symmetry): Hydrogen Bond Geometry of the Optimized Complexes[a]

		r(ON)	*r*(OH)	*a*(OHN)
l•1′	NO_2	327.7	229.0	162.8
l•2′	Cl	323.4	223.7	165.4
l•3′	H	322.4	222.4	166.1
l•4′	*t*Bu	321.6	221.3	166.9
l•5′	OCH_3	320.5	220.0	167.9

[a] Distances *r* in pm; angles *a* in degrees.

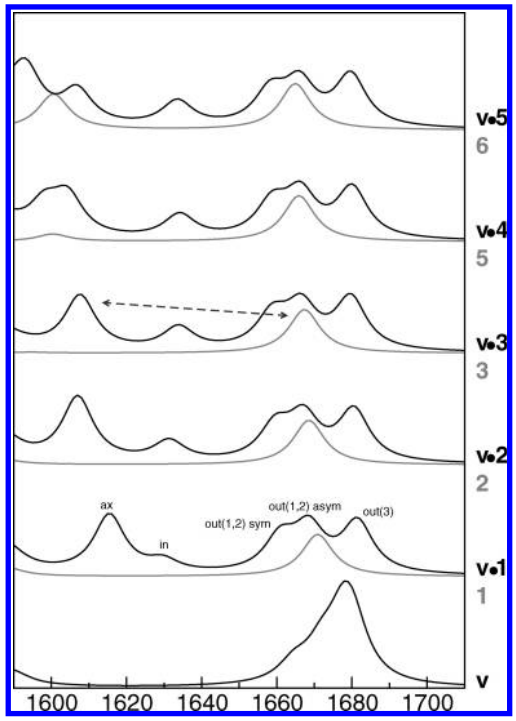

Figure 4. Calculated spectra in the region of 1600 to 1700 cm^{-1} displaying the carbonyl stretch bands. Gray: Axle spectra. The dashed arrow illustrates the shift of the axle's CO bands due to the complex formation.

The stronger individual hydrogen bonds E_{av}^{SEN} of the Vögtle-type pseudorotaxanes are reflected in shorter hydrogen bond distances (approximately 300 pm).[31]

4. Vibrational Analysis of the Vögtle-Type Pseudorotaxanes

In the following we will mainly focus on two modes, i.e. the carbonyl stretch vibration (1400−1700 cm^{-1}) and the NH stretch vibration (3300−3550 cm^{-1}).

4.1. Carbonyl Stretch Frequency Shifts. The carbonyl bands appear for both pseudorotaxane systems between 1600 and 1700 cm^{-1} in accordance with other work.[26,44,69] For simple secondary amides, these bands occur approximately 50−100 cm^{-1} higher in wavenumber.[37,39] Please note that these modes couple to other vibrations which was discussed in detail before.[37,38]

The Vögtle-type pseudorotaxane wheel in its 3-out-1-in conformation reveals one broad band at approximately 1680 cm^{-1} which is a superposition of four bands for the individual carbonyl groups. Each axle exhibits a carbonyl stretch band at ∼1670 cm^{-1}; see (blue) dotted arrow in Figure 4. Upon complex formation the latter are shifted to the region of 1610 cm^{-1}. The

Table 4. Vögtle-Type Complexes: Shifts $\Delta\nu$ of CO Stretch Vibrational Frequencies in [cm^{-1}][a]

	in av	$out_{1,2}$ sym va_1, va_2	$out_{1,2}$ asym va_1, va_2	ax av
v•1	−35	−9	−11	−56
v•2	−34	−11	−12	−61
v•3	−31	−11	−13	−59
v•4	−31	−12	−14	−62
v•5	−32	−12	−14	−58

[a] The sign of each shift is given by the difference of the complex minus the isolated molecule. "sym" and "asym" indicate the symmetry of the vibration (symmetric/asymmetric) for the coupled out_1 and out_2 vibration. "ax" gives the numbers due to the amide group of the axle. For definition of corresponding hydrogen bonds in third line, see Figure 2.

axle-wheel formation leads to a splitting of the one broad band, because hydrogen bond formation renders the four carbonyl groups so different that each of them can be detected by its own stretch mode; see Figure 4.

The behavior of the CO shifts becomes clearer upon inspection of Table 4. The large red shifts of the axle's carbonyl group is due to the hydrogen bonds which are accepted by that particular carbonyl group (va_1 and va_2) and which are the major cause for the host−guest interaction; see also ref 31. In line with previous experimental work,[26] small shifts are observed for the out_1 and out_2 carbonyl groups, although they are not directly involved in hydrogen bonding. It should be noted here that substituent effects are hardly detectable in the carbonyl shifts.

Our calculated CO shifts compare well with the values of Rijs et al.[26] For the two investigated rotaxanes they found shifts of −40 and −41 cm^{-1}. Experimental and theoretical studies concerning the influence of the solvent effect on the vibrational frequencies of a rotaxane molecule were carried out recently.[28] It was found that wavenumbers of the CO groups residing inside the macrocycle remain unaffected by the solvent polarity. However, a correlation between solvent acceptor number and CO frequency could be observed in this earlier study.[28] Calculated shifts from Table 1 of ref 37 range from −10 to −56 cm^{-1} in the formamide decamer, and it is approximately −15 cm^{-1} in the formamide dimer.[37] Compared to the present calculated results (Table 4) this indicates a high cooperativity of the investigated pseudorotaxanes.

4.2. NH Stretch, NH Bend, and CH Stretch Frequency. In agreement with literature,[37,44,69] the NH stretch bands are detectable in the approximate region 3350 to 3500 cm^{-1}; see Figure 5. These bands are not very intense for the isolated thread and macrocycle; see in Figure 5 bottom spectrum of **1**. However, the bands become more intense when a complex is formed. For example, compare the gray spectrum of **3** in Figure 5 with the black spectrum of **v•3** (blue arrow). Again, this was observed before for example at formamide or at 4-pyridone chain clusters.[37,38] This intensity increase goes along with a very large red shift (up to −136 cm^{-1} in case of the Vögtle-type pseudorotaxane); see Figure 5 and Table 3. In the following we first concentrate on the Vögtle-type pseudorotaxane. Again we only show those NH groups in Table 5 for which shifts are detected; these are the two NH groups ($out_{1,2}$) involved in the 2-fold hydrogen bond and the NH group from the axle. While the asymmetric $out_{1,2}$ stretch is very intense the symmetric mode appears only with low intensity.

It is striking that the individual hydrogen bond interaction energies (Table 1) as well as the shifts in Table 5 parallel the substituent effects. A larger shift corresponds to a stronger

(69) Fanti, M.; Fustin, C.; Leigh, D. A.; Murphy, A.; Rudolf, P.; Caudano, R.; Zamboni, R.; Zerbetto, F. *J. Phys. Chem. A* **1998**, *102*, 5782–5788.

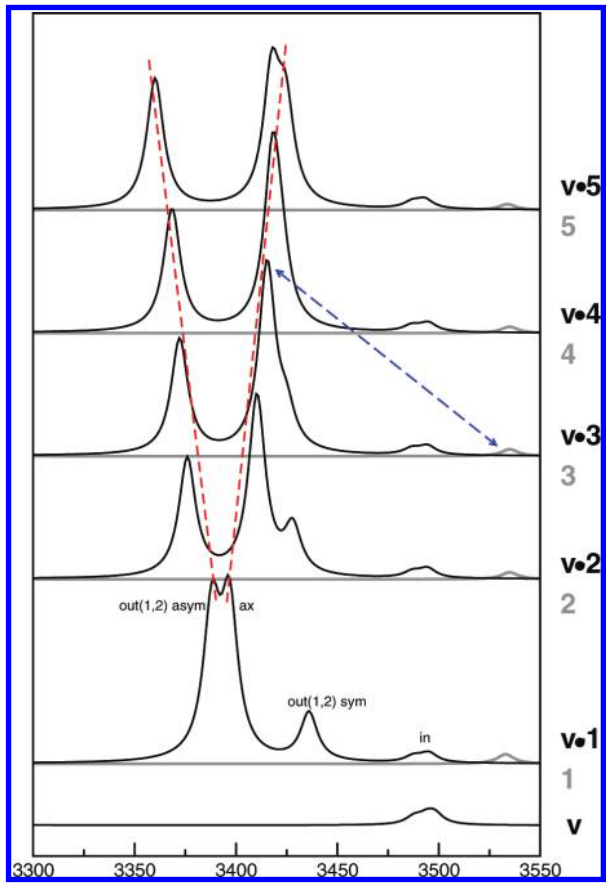

Figure 5. Calculated spectra in the region of 3300 to 3550 cm^{-1} displaying the NH stretch bands. The dashed arrow illustrates the shift of the axle's NH bands due to the complex formation.

Table 5. Vögtle-Type Complexes: Shifts $\Delta\nu$ of the NH Stretching Modes in $[cm^{-1}]$[a]

	$out_{1,2}$ sym	$out_{1,2}$ asym	ax
v•1	−62	−109	−136
v•2	−70	−121	−124
v•3	−74	−125	−120
v•4	−80	−129	−113
v•5	−81	−137	−110

[a] For a definition of the labels, see Figure 2. The corresponding spectra are shown in Figure 5.

individual hydrogen bond. If we compare the shift ($out_{1,2}$) of the stronger 2-fold hydrogen bond (third column in Table 5) to the partial charges calculated for the axle carbonyl oxygen in ref 31 (decreasing from **v•1** −0.747 *e* to **v•5** −0.765 *e*), we see the same correspondence. With increasing partial charge, a larger charge transfer from the carbonyl oxygen into the NH σ^* orbital of the hydrogen-bond donor occurs, and as a result the NH bond is weakened.[70] Therefore they are easier to excite and larger red shifts are observed. The NH stretching mode shifts reflect the substitution pattern and the behavior of the individual hydrogen bonds much more closely and in a more pronounced way than the CO shifts. The larger sensitivity of the NH stretch mode shift as compared to the CO frequency shift was previously observed for several clusters which form hydrogen bonds between amide groups.[37,38] For the axle the increasing

(70) Reed, A. E.; Curtiss, L. A.; Weinhold, F. *Chem. Rev.* **1988**, *88*, 899–926.

Table 6. Vögtle-Type Complexes: Shifts $\Delta\delta$ of the NH Bending Modes in $[cm^{-1}]$[a]

	$out_{1,2}$ sym	$out_{1,2}$ asym	ax
v•1	16	12	43
v•2	18	13	42
v•3	19	14	41
v•4	10	24	50
v•5	10	24	54

[a] For illustration of the labeling see Figure 2.

hydrogen bond strength corresponds with a growing NH shift. The same is observed for the macrocycle donating NH hydrogen bonds. If NH stretch mode shifts are detectable they will thus provide a solid measure for individual hydrogen bond strengths.

Blue shifts are also found,[37] namely in the constitution of NH bend modes which appear in the region of 1450 to 1550 cm^{-1} approximately. These shifts are as large as 50 cm^{-1} (see Table 6) and follow similar trends as the NH stretch modes but much less pronounced. This was previously observed for the calculated spectra of formamide chain clusters.[37] As an explanation of this phenomenon the polarization of the π-system that accompanies the cooperative interaction of the hydrogen bond was given for formamide chain clusters.[37] Increasing CO bond length goes along together with the loss of its π -character, while the CN bond contracts as it acquires more π-character.[37] In the first measured gas-phase rotaxane spectra NH bending modes were also detected. For rotaxane **2** of ref 26 a blue shift of 20 cm^{-1} was observed. In this rotaxane no hydrogen bond from an axle's NH group to the wheel is formed.[26]

There is a very weak hydrogen bond contact between the acceptor oxygen of the thread and the middle CH group of the macrocycle's benzyl group which contains the donating NH groups. This weak contact is reflected in blue shifts up to 20 cm^{-1} for the corresponding CH stretch mode; for details see Supporting Information and refs 44 and 45.

Comparing the NH shifts (Table 5) to the formamide chain decamer (−10 to −56 cm^{-1}) and the dimer (−10 cm^{-1}) reveals again that the pseudorotaxanes are highly cooperative systems.[37] Interestingly, these shifts were calculated to be as large as −500 cm^{-1} in 4-pyridone clusters.[38] The coupling of the CO stretch could be attributed to the cooperative hydrogen bonding rather than to through-space transition dipole coupling. In comparison CH vibrations were found to be too weak to alter the appearance of the NH stretch modes.[38] This might be a possible explanation for the more apparent substituent effect in the NH mode.

5. Detailed Assignment of the Leigh-Type Pseudorotaxane Spectrum

While the Vögtle-type pseudorotaxanes exhibit no symmetry, i.e. belong to the point group C_1, we can determine C_{2h}-symmetry for the Leigh-type pseudorotaxanes.

5.1. Wheel. In Table 7 we list the normal modes of the Leigh-type wheel. There are four NH and four CO groups in the wheel, yielding each four local stretching modes for CO and NH plus four NH bending modes. These four local modes couple to four normal modes comprising all four irreducible representations of the point group C_{2h}. Hence two of them are IR active (u) while the gerade normal modes are Raman active (strict exclusion principle). It is apparent from the numbers in Table 7 that averaging over all normal modes (neglecting symmetry assigment) is justified.

Table 7. Leigh-Type Complexes (C_{2h} Symmetry): Normal Modes of the Wheel **I**[a]

mode	symmetry	cm^{-1}	I (IR)	I (Raman)
ν_1 (NH)	b_u	3538	19	–
ν_1 (NH)	a_g	3538	–	247
ν_1 (NH)	a_u	3536	15	–
ν_1 (NH)	b_g	3536	–	25
ν_1 (CO)	b_u	1668	447	–
ν_1 (CO)	a_g	1669	–	150
ν_1 (CO)	a_u	1663	475	–
ν_1 (CO)	b_g	1662	–	22
δ_1 (NH)	b_u	1482	721	–
δ_1 (NH)	a_g	1484	–	65
δ_1 (NH)	a_u	1487	134	–
δ_1 (NH)	b_g	1484	–	54

[a] ν denotes the stretch frequency [cm^{-1}], and δ [cm^{-1}] is the bending frequency. IR intensity in [km/mol], Raman activity in [$Å^4$/amu]; excitation wavelength is set to 514.5 nm (Ar laser).

Table 8. Leigh-Type Complexes (C_{2h} Symmetry): Normal Modes of the Axle Molecules **1′**–**5′** in [cm^{-1}][a]

	$\nu_2^{b_u}$ (CO)	I (IR)	$\nu_2^{a_g}$ (CO/CC)	I (Raman)	$\nu_3^{a_g}$ (CO/CC)	I (Raman)
1′	1675	255	1695	67	1630	14 425
2′	1664	293	1686	225	1627	15 007
3′	1666	288	1687	229	1628	9510
4′	1662	297	1685	409	1627	13 167
5′	1656	299	1679	730	1627	9958

	$\delta_2^{b_u}$ (NH)	I (IR)	$\delta_2^{a_g}$ (NH)	I (Raman)
1′	1508	506	1515	3578
2′	1489	693	1492	9983
3′	1503	470	1506	4713
4′	1497	430	1487	5099
5′	1494	771	1496	20 036

[a] IR intensity in [km/mol], Raman activity in [$Å^4$/amu], excitation wavelength is set to 514.5 nm (Ar laser).

Table 9. Leigh-Type Complexes (C_{2h} Symmetry) First Part: CO and CC Stretch Modes of the Complex in [cm^{-1}][a]

	$\nu_1^{b_u}$ (CO)	I (IR)	$\Delta\nu$	$\nu_2^{b_u}$ (CO)	I (IR)	$\Delta\nu$
		wheel			axle (HB)	
I•1′	1661	354	−7	1631	367	−44
I•2′	1661	406	−7	1618	397	−46
I•3′	1660	397	−8	1617	392	−49
I•4′	1659	405	−9	1613	419	−49
I•5′	1659	404	−9	1609	321	−47

	$\nu_1^{a_g}$ (CO)	I (Raman)	$\Delta\nu$	$\nu_2^{a_g}$ (CO)	I (Raman)	$\Delta\nu$
		−wheel+axle			wheel+axle	
I•1′	1671	964	–	1662	137	–
I•2′	1664	1467	–	1660	683	–
I•3′	1664	1188	–	1660	350	–
I•4′	1659	811	–	1662	219	–
I•5′	1654	4186	–	1660	618	–

[a] IR intensity in [km/mol], Raman activity in [$Å^4$/amu], excitation wavelength is set to 514.5 nm (Ar laser).

Table 10. Leigh-Type Complexes (C_{2h} Symmetry) Second Part: CO,CC Stretch Modes of the Complex in [cm^{-1}][a]

	$\nu_3^{a_g}$ (CO)	I (Raman)	$\Delta\nu$
		axle (HB)	
I•1′	1615	9663	−15
I•2′	1609	8037	−18
I•3′	1608	4168	−20
I•4′	1609	1096	−18
I•5′	1614	45	−13

	$\nu_1^{a_u}$ (CO)	I (IR)	$\Delta\nu$	$\nu_1^{b_g}$ (CO)	I (Raman)	$\Delta\nu$
		wheel			wheel	
I•1′	1655	503	−8	1655	7	−7
I•2′	1654	515	−9	1654	8	−8
I•3′	1653	520	−10	1653	8	−9
I•4′	1652	516	−11	1652	8	−10
I•5′	1655	455	−8	1654	14	−8

[a] IR intensity in [km/mol], Raman activity in [$Å^4$/amu], excitation wavelength is set to 514.5 nm (Ar laser).

5.2. Axles. In Table 8 we give the modes of the isolated axle molecules **1′**–**5′**. For the CO group we obtain now three normal modes, because the gerade CO stretch mode couples with the gerade CC stretch mode. The ungerade CO stretch normal mode does not significantly couple with any other ungerade mode in this wavenumber range. There is only a slight coupling with the NH bending mode. The NH bending modes of the axle are reflected in two IR and Raman active modes coupling with each other but not strongly with other vibrations. The substituent effect is clearly reflected in the wavenumbers of the $\nu_2^{b_u}$ (CO) mode.

5.3. Complexes. 5.3.1. Carbonyl Stretch Frequency Shifts. In Tables 9 and 10 we summarize the CO modes of the Leigh-type complexes. Only the $\nu_1^{a_g}$ (CO) and $\nu_2^{a_g}$ (CO) a_g modes show strong coupling of wheel and axle vibrations, see Figure 6. Therefore we do not provide frequency shifts. The $\nu_3^{a_g}$ (CO) a_g mode in Table 10 remains conserved if compared to the corresponding axle mode but shifts because of the hydrogen bond. The normal modes of b_u symmetry from axle and wheel should couple (first block in Table 9), but they remain uncoupled because the axle takes part in hydrogen bonding with the CO group and the wheel does not with its CO group. Although the substituent effect is still clearly reflected in the wavenumbers of the $\nu_2^{b_u}$ (CO) mode, the corresponding shift does not show any trend according to the strength of the hydrogen bond. This is obvious, because the substitution effect is the same in the isolated axle and the complex. A different situation has to be expected for the comparison between the isolated wheel and the complex. At the wheel there is no substituent effect, but upon complex formation such an effect is added. Therefore, the overall effect is present in the wheels' NH shifts and not in the CO shifts of the axle as already discussed for the Vögtle type complex and as can be seen in a later section where the NH shifts are discussed.

The Leigh-type pseudorotaxanes shifts are also presented in Tables 9 and 10. For these complexes we observe small shifts (up to 12 cm^{-1}) for the carbonyl groups which are not directly involved in hydrogen bonding as well. Larger shifts are found for the CO groups that are engaged in hydrogen bonding. The shifts are smaller than those for the Vögtle-type complexes; i.e. values up to −49 cm^{-1} are calculated.

5.3.2. NH Stretch Frequency Shifts. In Table 11, the NH stretch frequencies are summarized which relate to the individual hydrogen bonds. In this case the substituent effect is again reflected in the trend of the shift. As in the case of the Vögtle-type pseudorotaxanes, it is on the order of ca. 30 cm^{-1}; see Table 11.

The analysis of a simulated catenane spectrum[71] with the same macrocycle as our studied Leigh-type pseudorotaxane revealed that such shifts are entirely due to the interlocked

(71) Fustin, C.; Leigh, D. A.; Rudolf, P.; Timpel, D.; Zerbetto, F. *ChemPhysChem* **2000**, *2*, 97–100.

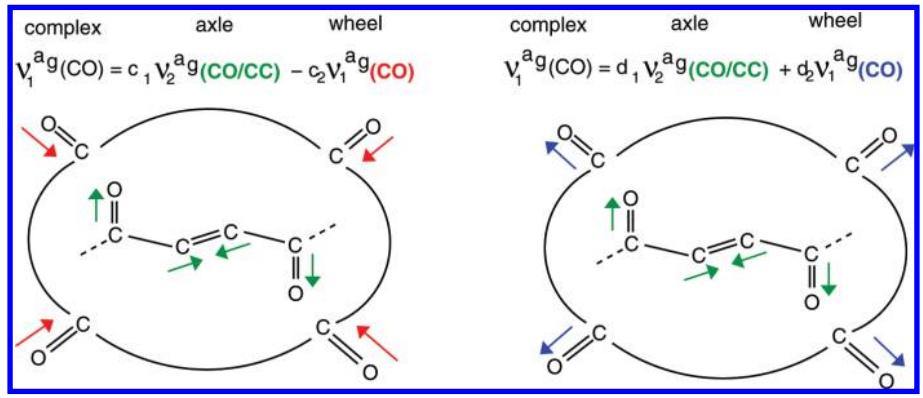

Figure 6. Illustrated a_g vibrational modes ($\nu_1^{a_g}$ (CO) and $\nu_2^{a_g}$ (CO)) of the Leigh-type complex and the coupling between modes from the axle and the wheel.

Table 11. Leigh-Type Complexes (C_{2h} Symmetry): NH Stretch Modes of the Complex in [cm^{-1}][a]

		ν	I (IR)	$\Delta\nu$	ν	I (IR)	$\Delta\nu$
			a_u			b_u	
l	–	3536	15	–	3538	19	–
l•1′	NO_2	3473	127	−63	3476	211	−62
l•2′	Cl	3460	167	−76	3463	269	−75
l•3′	H	3452	176	−84	3456	278	−82
l•4′	*t*Bu	3449	185	−87	3453	305	−85
l•5′	OCH_3	3442	207	−94	3447	326	−91
		ν	I (Raman)	$\Delta\nu$	ν	I (Raman)	$\Delta\nu$
			b_g			a_g	
l	–	3536	25	–	3538	247	–
l•1′	NO_2	3473	67	−63	3476	831	−62
l•2′	Cl	3459	67	−77	3464	1077	−74
l•3′	H	3451	64	−85	3456	831	−82
l•4′	*t*Bu	3448	71	−88	3453	1154	−85
l•5′	OCH_3	3442	71	−94	3447	1434	−91

[a] IR intensity in [km/mol], Raman activity in [Å^4/amu]; excitation wavelength set to 514.5 nm (Ar laser).

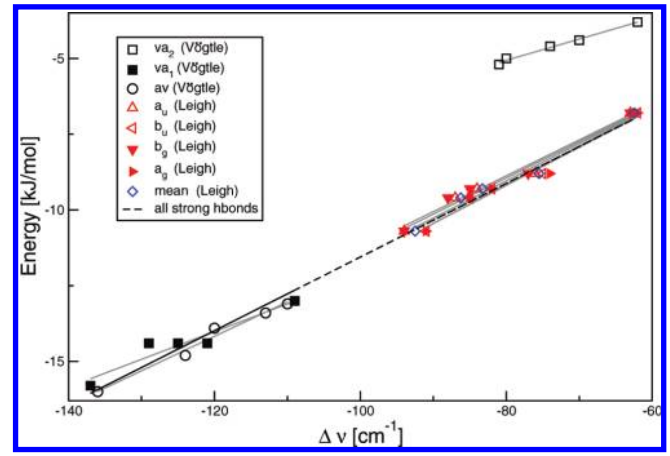

Figure 7. Individual hydrogen bond energy in [kJ/mol] plotted against the individual shifts $\Delta\nu$ in [cm^{-1}] of the calculated NH stretch mode.

molecular architecture which provides a suitable geometry for intercomponent hydrogen bonds.

5.4. Correlation between Energy and Frequency Shift. From the results discussed so far we can draw two major conclusions:

• Due to the compensating contributions from the two different types of hydrogen bonds (wheel-C═O···H─N-axle vs wheel-N─H···O═C-axle), it is not straightforward to correlate the vibrational modes with the total interaction energy in the case of the Vögtle-type pseudorotaxanes. Rather, the individual hydrogen bonds must be considered separately. However, for the Leigh-type compounds the correlation of the vibrational modes with the individual as well as with the total energy is appropriate, because all individual hydrogen bonds belong to the same type (wheel-C═O···H─N-axle). For both complexes the CO-shift does not reflect the substitution pattern as it is accounted for in both the isolated axle and the complex.

• The largest frequency shifts have been observed for the NH stretch vibration. Furthermore, these shifts reflect the substitution pattern, because the difference between the wheel and the complex is rooted in the hydrogen bond as well as in the added substituent effect. Consequently, this mode provides the most reliable data for a correlation with individual hydrogen bond strengths.

A connection between the proton stretching vibration red shift and hydrogen bond properties has been drawn already in 1937.[72,73] Later Rozenberg et al.[74] correlated this shift to the length of the hydrogen bond ($\Delta\nu \propto r^{-6}$) in polycrystalline amino acids and peptides.[72] With the aid of Iogansen's "intensity rule" it is furthermore possible to establish a relationship between energies and spectra.[75] Dannenberg and co-workers discussed such relationships at the increasing chain length of different amide containing chain clusters.[37,38] A correspondence between theoretically derived frequency shifts and calculated energies was previously established for some simpler 2-fold hydrogen-bonded rotaxane mimics.[44]

Figure 7 shows the results of a linear regression analysis between the individual hydrogen bond energies and the NH frequency shifts. While the shifts for the Vögtle-type pseudorotaxanes are shown individually, the shifts of the Leigh-type molecules are presented both individually (red) and as the average (blue) in Figure 7, because the individual energy for each substituent is the same for the different symmetries.

In Table 12, the results of the linear regressions are shown. We observe that for all calculated energies the slope is positive and the correlation coefficients are close to one, thus indicating the practicability of these linear regressions. Interestingly, the NH shift E^{SEN} relationship of the Leigh-type pseudorotaxanes complement the strong individual hydrogen bonds of the Vögtle-type pseudorotaxanes in a perfect way. In addition Figure 7

(72) Badger, R. M.; Bauer, S. H. *J. Chem. Phys.* **1937**, *5*, 839–851.
(73) Badger, R. M. *J. Chem. Phys.* **1940**, *8*, 288–289.
(74) Rozenberg, M.; Shoham, G.; Reva, I.; Fausto, R. *Phys. Chem. Chem. Phys.* **2005**, *7*, 2376–2383.
(75) Iogansen, A. V. *Spectrochim. Acta A* **1999**, *55*, 1585–1612.

Table 12. Results of the Linear Regressions for Figure 7[a]

shifts	E	m	Δm	b	Δb	cc
av(Vögtle)	E_{av}^{SEN}	0.091	0.016	−3.0	2.0	0.96
va_1(Vögtle)	$E_{va_1}^{SEN}$	0.114	0.009	−0.5	1.1	0.99
va_2(Vögtle)	$E_{va_2}^{SEN}$	0.070	0.004	0.5	0.3	1.00
a_u(Leigh)	E^{SEN}	0.119	0.010	0.6	0.8	0.99
b_u(Leigh)	E^{SEN}	0.128	0.010	1.1	0.8	0.99
b_g(Leigh)	E^{SEN}	0.118	0.010	0.6	0.9	0.99
a_g(Leigh)	E^{SEN}	0.126	0.012	0.9	1.0	0.99
all(Leigh)	E^{SEN}	0.123	0.011	0.8	0.9	0.99
all ∉ va_2(Vögtle)	E_{all}^{SEN}	0.122	0.004	0.6	0.4	0.99
all(Leigh)	ΔE^{calc}	0.709	0.048	7.9	3.9	0.99

[a] E: The energies in [kJ/mol] at which the data were fitted; m: Slope; Δm: Standard error of m in [kJ cm/mol]; b: Intercept with error Δb in [kJ/mol], and cc: Correlation coefficient.

Table 13. Calculated Shifts in [cm^{-1}],[45] Different Energies Obtained from the Electronic Structure Calculation ΔE^{calc} and the SEN Analysis,[55,64,65] and Values from the Fit with the Shifts for the Different Coconformations of Complex **v•3** in [cm^{-1}][a]

	ν(av)	ν(va_1)	ν(va_2)
v•3	−120	−125	−74
v•3a	−	−104	−86
v•3b	−	−91	−
v•3c	−	−180	−

	ΔE^{calc}	E_{av}^{SEN}	$E_{va_1}^{SEN}$	$E_{va_2}^{SEN}$	$\sum E^{SEN}$
v•3	−36.5	−13.9	−14.4	−4.6	−32.9
v•3a	−12.2	−	−10.9	−8.3	−19.2
v•3b	−4.7	−	−14.0	−	−14.0
v•3c	−16.2	−	−23.0	−	−23.0

	E_{av}^{fit}	$E_{va_1}^{fit}$	$E_{va_2}^{fit}$	$\sum E^{fit}$
v•3	−14.0	−14.7	−4.7	−33.4
v•3a	−	−12.1	−5.5	−17.6
v•3b	−	−10.5	−	−10.5
v•3c	−	−21.4	−	−21.4

[a] With the exception of E $(va_2)_{fit}$ (inserted in va_2 (Vögtle)), all energies were calculated with the equation for all ∉ va_2 (Vögtle). All energies in kJ/mol.

clearly shows that for such a regression analysis a distinction between weak and strong hydrogen bonds has to be made. A possible way to detect this is given by the intensity; see Figure 5. The va_2 ($out_{1,2}$ (sym)) is much less intense than the other modes.

In order to test the obtained linear regression, a data set not belonging to the fit set is applied to this regression. To evaluate our results in this way, three different coconformers of complex **v•3** will serve as a test set; see also Figure 2 and ref 45 where these structures are depicted. They are labeled **v•3a**−**v•3c** and can be understood as different intermediates of the threading process to the extent that as from **v•3c** to **v•3a** the axle comes closer and closer to its final arrangement in **v•3**. Table 13 gives an overview of the different interaction energies predicted for these structures.[45]

In the second data block of Table 13 the results of the SEN analysis are shown. On the one hand it might be reasonable that the sum of the individual hydrogen bond energies deviates from ΔE^{calc}, because the SEN energy only describes the hydrogen bond and no repulsive or other attractive interactions. On the other hand this can also be due to the fact that the SEN analysis has to be treated with care when strained hydrogen bonds are involved (see ref 64 for an extensive discussion); i.e., the SEN method only serves as a semiquantitative analysis.[52]

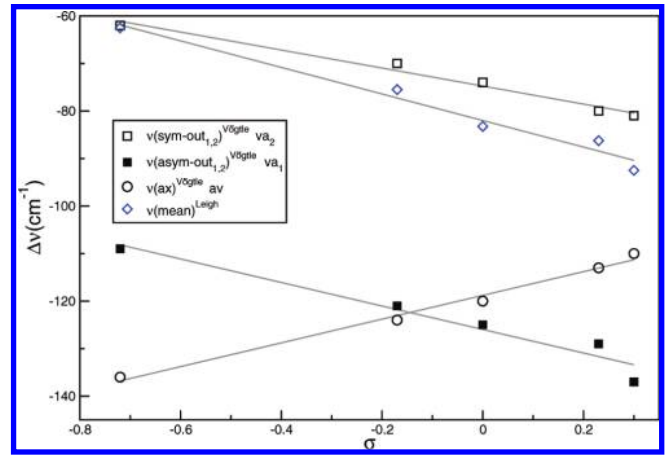

Figure 8. The shifts $\Delta\nu$ in [cm^{-1}] of the calculated NH stretch mode from Table 5 and the average from Table 11 plotted against the Hammett parameter.

Application of the individually fitted regression curves from Figure 7 leads to the numbers listed in the last block of Table 13. These results demonstrate that our fits (E^{fit}) of the individual hydrogen bond energies (E_{av}^{SEN}, $E_{va_1}^{SEN}$, $E_{va_2}^{SEN}$) reproduce the individual hydrogen bonds well enough to roughly mirror the present SEN energy trend. This example clearly indicates that it might be worthwhile to apply a fit analysis of energies calculated with high-quality methods to frequency shifts in which anharmonicities do not play an important role and in which a single hydrogen bond is the only contribution to the interaction energy. In this way the estimation of the individual hydrogen bond energy via a frequency shift from theoretical calculations or from an experimental measurement would be possible. This is especially important as the individual hydrogen bond energies are not observable. However, the IR spectrum of a substance and thus the frequency shift can be measured. Given that the coupling of modes is not too strong, the frequency shifts may well be a valuable measure for individual hydrogen bond energies.

The total energy can also be correlated with the shifts of Leigh-type pseudorotaxanes. In the last line of Table 12 the results of this fit are shown. Although the trend is reflected in the total interaction energy, it is obvious that a correlation with the individual hydrogen bond energy is much easier. It should be noted that we obtained intercepts with the linear regression that are larger than zero.

5.4.1. Hammett Parameters and Frequency Shifts. Turning now to the interplay of the substituent, hydrogen bond, and spectrum, we correlate Hammett's substituent parameters with the NH stretching shifts.[46]

Figure 8 shows the results of the correlation between the Hammett parameters and NH stretch frequency shifts. Clearly, the shifts of the NH stretch frequency provide an excellent measure for the substituent effect. The results of the regression are given in Table 14, and the quality of the correlation coefficients again demonstrates how well the substituent effects correlate with changes in this particular NH stretch mode.

Please note that due to the symmetry the mean values of the shifts were fitted for the Leigh-type complexes. Thus it is appropriate to postulate not only a relationship between

Table 14. Results of the Linear Regressions for Fig 8[a]

$\Delta\nu$	type	m	Δm	b	Δb	cc
ax	Vögtle	24.980	1.532	−118.8	0.6	0.99
sym-out$_{1,2}$	Vögtle	−18.944	1.554	−74.8	0.6	−0.99
asym-out$_{1,2}$	Vögtle	−24.737	3.347	−126.0	1.2	−0.97
mean	Leigh	−27.929	2.672	−82.0	1.0	−0.99

[a] m: Slope; Δm: Standard error of m; b: Intercept with error Δb, and cc: Correlation coefficient. All parameters in [cm^{-1}].

hydrogen bond and frequency but also between hydrogen bond strength (tuned by the substituent) and the frequency shift.

Discussion and Conclusion

We presented a theoretical investigation of the IR spectra for two differently substituted pseudorotaxanes, with a focus on the substituent effect, hydrogen bond, and IR frequency shifts, to provide a tool for the determination of individual amide hydrogen bond strengths on the basis of frequency shifts.

We found for both pseudorotaxanes large red shifts for the axle carbonyl stretch of approximately the same size (Vögtle: −60 cm^{-1}; Leigh: −50 cm^{-1}), which are more or less affected by the axle substituent by up to −10 cm^{-1}. As previously discussed, the total binding energy does not vary due to the compensating effect of the substitution pattern on hydrogen bond acceptor and donor groups, both present in the Vögtle-type pseudorotaxanes.[31] Furthermore the carbonyl group from the axle as well as the complex includes the substitution effect. Thus, the frequency difference between both does not reflect the substitution effect. Therefore, the carbonyl fit is not suitable to detect individual hydrogen bonds or total binding energies for this example. Although trends in the total interaction energies are observed for the Leigh-type pseudorotaxane, we refrained from fitting energies to carbonyl related spectroscopic data. As previously observed by the Buma group, we find the peculiar shifts for those CO groups that point outside of the macrocycle and are not directly involved in the 2-fold hydrogen bond.[26]

Two blue-shifted modes of Vögtle-type pseudorotaxanes were shortly discussed, namely the NH bending mode in the region 1480 to 1530 cm^{-1} and the CH stretching mode in the region 3090 to 3110 cm^{-1}. An explanation of this was previously provided by the Dannenberg group who ascribed this to a change in π-character of CO and NH bonds.

The largest shifts were found in the case of the NH stretch modes with values of up to −137 cm^{-1} for the Vögtle-type pseudorotaxanes and −94 cm^{-1} for the Leigh-type pseudorotaxanes. Because these shifts reflect the trends in the individual hydrogen bond energies as estimated in terms of the SEN method,[55] they were applied in a linear regression treatment to obtain a correlation between the NH stretch shift and individual hydrogen bond energy. Relating the individual shifts to the individual hydrogen bonds by linear regression resulted in correlation coefficients very close to one. Interestingly, weak and strong hydrogen bonds had to be separated (distinguished by significantly different IR intensities), and the Leigh-type pseudorotaxane numbers completed the linear dependence in a very accurate way. The subsequent calculation of individual energies with the aid of the linear regression for test systems of similar complexity led to a good agreement with the individual energies obtained via the SEN method. Finally, because the substituent effects can be quantified with the aid of the well-known Hammett parameters, we also fitted experimentally determined Hammett parameters to the frequency shifts and found an excellent correlation between them. Thus we could establish a linear relation between substitution effect (i.e., strength of the hydrogen bond in similar complexes), hydrogen bond, and frequency. In accordance with experimental work,[74,75] we altogether found that IR spectra are able to provide a measure of the strengths of individual hydrogen bonds which are not separately observable otherwise and which are thus not easy to detect in a direct way from a theoretical point of view.[55]

Acknowledgment. This article is dedicated to Professor Fritz Vögtle on the occasion of his 70th birthday. Financial support by DFG for the collaborative research centers SFB 765 "Multivalency" at the Free University of Berlin and the SFB 624 "Templates" at the University of Bonn is gratefully acknowledged.

Supporting Information Available: Table of CO stretch modes; table of NH stretch modes; table of NH bend modes; table of CH stretch modes; tables containing the Cartesian coordinates and total energies of the stationary points of all complexes. This material is available free of charge via the Internet at http://pubs.acs.org.

JA902628N